

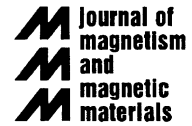


ELSEVIER

Available online at [www.sciencedirect.com](http://www.sciencedirect.com)

SCIENCE @ DIRECT®

Journal of Magnetism and Magnetic Materials 293 (2005) 80–86



[www.elsevier.com/locate/jmmm](http://www.elsevier.com/locate/jmmm)

# Magnetic properties of bacterial magnetosomes as potential diagnostic and therapeutic tools

Rudolf Hergt<sup>a,\*</sup>, Robert Hiergeist<sup>a</sup>, Matthias Zeisberger<sup>a</sup>, Dirk Schüler<sup>b</sup>,  
Udo Heyen<sup>b</sup>, Ingrid Hilger<sup>c</sup>, Werner A. Kaiser<sup>c</sup>

<sup>a</sup>*Institut für Physikalische Hochtechnologie e.V., P.O. Box 100239, D-07702 Jena, Germany*

<sup>b</sup>*Max-Planck-Institut für Marine Mikrobiologie, Celsiusstr. 1, D-28865 Bremen, Germany*

<sup>c</sup>*Institut für Diagnostische und Interventionelle Radiologie der Friedrich-Schiller-Universität Jena, Forschungszentrum Lobeda POB D-07740 Jena, Germany*

Available online 5 March 2005

## Abstract

Suspensions of bacterial magnetosomes are investigated with respect to magnetic losses. Mean core diameter of about 30 nm results from TEM, XRD and magnetic analysis. Specific loss power is determined from hysteresis loops, susceptibility spectra and calorimetry with a maximum value of 960 W/g at 410 kHz and field amplitude 10 kA/m. Results may be understood by relaxation effects on hysteresis.

© 2005 Elsevier B.V. All rights reserved.

*PACS:* 75.50.Tt; 75.50.Mm; 75.40.Gb; 75.60.Jk; 75.60.Lr; 87.54.Br

*Keywords:* Nanoparticles; Ferrofluids; Magnetosome; Brown relaxation; Néel relaxation; Magnetic susceptibility; AC losses; Magnetic hyperthermia

## 1. Introduction

Magnetotactic bacteria are capable of synthesising magnetosomes, the core of which consist of nano-sized crystals of magnetic iron oxide. Under controlled synthesis conditions uniform particles

of 20–45 nm core diameter may be produced which are of interest for a number of potential applications recently suggested [1]. However, the magnetic and structural properties of magnetosomes have been insufficiently characterised up to now, mainly because of the unavailability of significant amount of material. By a new method the mass production of magnetosomes from the bacterium *Magnetospirillum gryphiswaldense* could be established [2].

One of the potential application areas of magnetosomes is magnetic particle hyperthermia

\*Corresponding author. Department of Magnetics, IPHT Jena, Albert-Einstein-Str. 9, 07745 Jena, Germany. Tel.: +49 3641 206133; fax: +49 3641 206199.

E-mail address: [hergt@ipht-jena.de](mailto:hergt@ipht-jena.de) (R. Hergt).

(MPH) reviews of which were given, e.g. by Moroz et al. [3], Andrä [4], and Hilger et al. [5]. As pointed out recently [6] an enhancement of specific heating power is of importance for reducing the useful dosage applied to the tumour. By this way a gain in reliability of MPH as tumour therapy is expected. Previous investigations on the suitability of magnetic nanoparticles for MPH [7,8] have shown that for the biocompatible magnetic iron oxides (magnetite and maghemite) a core size range above about 20 nm diameter is advantageous with respect to large specific heating power. Therefore, magnetosomes are of particular interest for testing their suitability for application in MPH tumour therapy. Magneto-liposomes were previously used by Shinkai et al. [9] for MPH. There, magnetite cationic liposomes were prepared by using commercial magnetite in difference to the bacterially synthesised magnetosomes investigated in the present paper. The authors reported remarkable findings of heating induced immunity effects. However, the specific heating power of the liposomes is not given explicitly in that paper. In the present paper first results of structural and magnetic characterisation of magnetic nanoparticles produced by magnetotactic bacteria are reported. By measuring different contributions of magnetic losses by means of alternative methods it is shown that the present magnetosomes are capable of delivering extremely large heating power which may be of interest for MPH.

## 2. Preparation and structural data

Bacterial magnetosomes of the type investigated in the present paper are synthesised in nature by magnetotactic bacteria *Magnetospirillum gryphiswaldense* under very special microaerobic conditions [1]. In order to cope with the difficulties to realise optimum conditions for bacteria growth and for magnetosome synthesis in laboratory a novel oxygen-controlled fermentor was developed, details of which were reported elsewhere [2]. Basing on a modified dual-vessel laboratory fermentor system equipped with automatic control of pH, temperature and dissolved oxygen concentration cultivation parameters for large magnetite

output were determined. As a result a maximum yield of 6.3 mg magnetite per litre and day was achieved. Magnetosomes were isolated from bacteria cells by a method combining ultracentrifugation and magnetic separation [10]. Finally, aqueous suspensions of magnetosomes were prepared for magnetic investigations described below.

Phase identification of the magnetic iron oxide of the magnetosomes was performed by X-ray diffraction (XRD). From diffraction patterns follows that the present magnetosomes contain as magnetic material a compound being intermediary between maghemite and magnetite. It seems that bacteria synthesise primarily magnetite which steadily transforms into maghemite after exposure to air. The observed XRD line broadening may be understood by particle size effects as may be deduced from comparison with data extracted from TEM imaging. From magnetisation measurements the concentration of magnetic iron oxide in the aqueous suspensions was determined as described in Section 3. Typically, a volume fraction of  $6.6 \times 10^{-4}$  is found assuming a mean value of mass density of particles of  $5.0 \text{ g/cm}^3$  according to the XRD results. This particle concentration is commonly considered as low enough to neglect particle interactions. However, transmission electron microscopy (TEM)—typical results of which are presented in Fig. 1—reveals that there are special effects of particle interactions. Typically, the low magnification image presented in Fig. 1a shows besides single magnetosomes, closed chains as well as agglomerations, too. The latter one may be artefacts due to preparation of TEM specimens while chains and isolated magnetosomes seem to be typical for the present suspensions. It is well known that magnetosomes in bacteria are arranged in straight chains (e.g. Ref. [1]). Reasonably, after isolation from bacteria those chains tend to form closed loops in suspension minimising in this way their magnetic stray field energy. Higher magnification (Fig. 1b) shows that the magnetosomes are bounded—at least partially—by crystallographic planes. Obviously, the particles are grown very near to equilibrium, in contrast to common chemical precipitation methods which result often in globular, poorly crystallised particles (cf. for instance

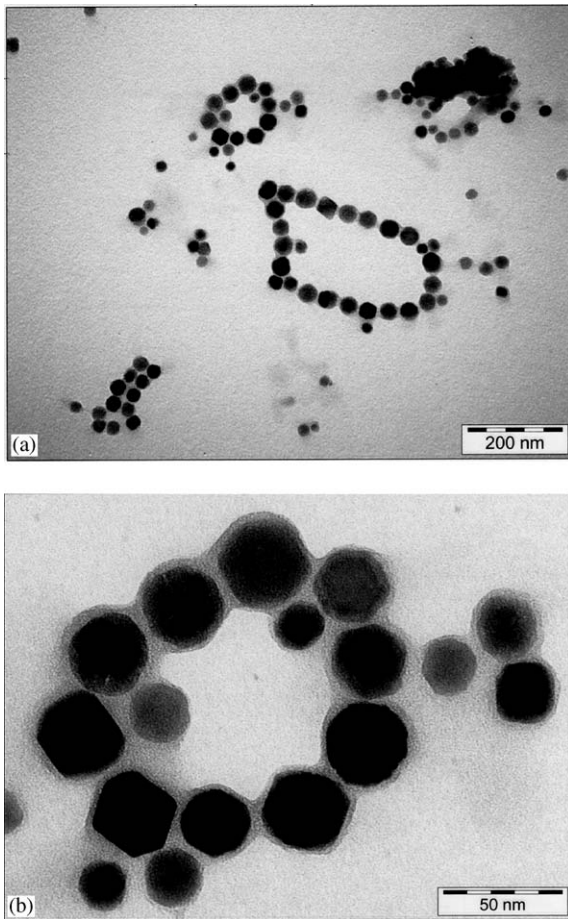


Fig. 1. Transmission electron micrographs of magnetic cores of magnetosomes at two different magnifications.

TEM images presented in Ref. [7,8]). In comparison to most wet chemical preparation techniques resulting in broad lognormal distributions (e.g. Ref. [8]) the size distribution of the magnetosomes is remarkably narrow. From TEM imaging follows for sample 1, results of which are shown in Fig. 1, a mean core size of 38 nm and mean square deviation of 5 nm. Taking into account the well known difficulties with sampling in TEM, mean core size was additionally determined from line broadening of X-ray diffraction which results in a mean core size of 39 and 30 nm, respectively, for samples 1 and 2 being investigated in the present paper.

For separating effects due to Néel or Brown relaxation magnetosomes were immobilised by suspension in liquid gelatine and subsequent solidifying using the temperature dependent sol–gel transition as described in detail previously [11]. Besides, textured samples were prepared by dissolving the magnetosomes in a liquid gelatine sol and cooling down below the sol–gel transition temperature (at  $\sim 30^\circ\text{C}$ ) in a constant magnetic field of 796 kA/m.

### 3. Magnetic properties

Magnetisation loops of as prepared aqueous suspensions of magnetosomes were measured by vibrating sample magnetometry (VSM) at room temperature. By comparing the measured saturation magnetic moment with theoretical saturation magnetisation [12] the content of magnetic iron oxide of the suspensions was estimated. There, according to results of XRD analysis a magnetic phase being intermediary between magnetite and maghemite was assumed having a mean saturation magnetisation of 450 kA/m. Using this value one finds a particle concentration of  $3.3\text{ mg/cm}^3$  which corresponds to a volume portion of  $6.6 \times 10^{-4}$  assuming a mean value of mass density of particles of  $5.0\text{ g/cm}^3$  according to above described XRD results. In addition to TEM and XRD, magnetic core size may be derived from magnetic measurements as demonstrated in Ref. [8]. If the magnetisation curve of a magnetic suspension is of the type of well known Langevin law, parameters of the size distribution which is assumed to be lognormal may be determined as shown by Chantrell et al. [13]. For aqueous suspensions of the presently investigated magnetosomes the coercivity at room temperature is very low (0.7 kA/m for samples 1 and 2). In contrast, by suspending magnetosomes in aqueous sol of gelatine with subsequent particle immobilisation by gelation [11] coercivity increases to 2.6 kA/m (sample 2). From magnetisation curves measured for liquid suspensions a mean core size diameter of 32 nm (sample 1) and 30 nm (sample 2) was determined following the procedure of Chantrell et al. [13]. These magnetically determined values are somewhat

smaller than above reported XRD results (39 and 30 nm, respectively) which confirms a tendency found already previously [7,8]. The standard deviation of the core size distribution resulting from magnetic analysis is 9 nm for sample 1 and 21 nm for sample 2. This is one of the most important differences between both samples being reflected in the data of specific loss power reported below. An indication for large specific loss power of the present particles is the measured large value of the initial DC-susceptibility of the particles in the order up to 1000 (particle susceptibility in SI units corrected for particle volume concentration) which let expect good heating effects of the particles in AC-magnetic fields according to previously found results for smaller particles (<18 nm mean core diameter) [7,8,14] and is confirmed by the measured specific loss power reported below. Magnetic losses of those particles being essentially smaller than the present ones could be well understood by the Debye theory of dispersion [15,16] as shown in Ref. [7]. For closer inspection, magnetic losses of liquid as well as solid suspensions of magnetosomes were investigated by three types of experiments: Quasistatic magnetic properties were analysed by measuring minor loops with a vibrating sample magnetometer (VSM). The small field amplitude dynamic response of the samples was investigated by measuring the complex susceptibility in a frequency range of 100 Hz–1 MHz. Finally, the specific loss power was determined calorimetrically for AC-field parameters being relevant for hyperthermia applications.

Magnetic losses were determined in dependence on field amplitude by measuring minor hysteresis loops of immobilised magnetosomes. Examples of minor loops measured by VSM for a particle suspension in gel are shown in Fig. 2 for sample 2. By integrating those minor loops hysteresis loss per cycle was determined in dependence on field amplitude. Results are shown in Fig. 3. For low amplitudes a square law is found which changes above about 2 kA/m to a third-order power law being typical for the Rayleigh regime [17] and reported previously for small particles [18]. The second-order power law at small amplitudes represents the linear regime tested with AC-

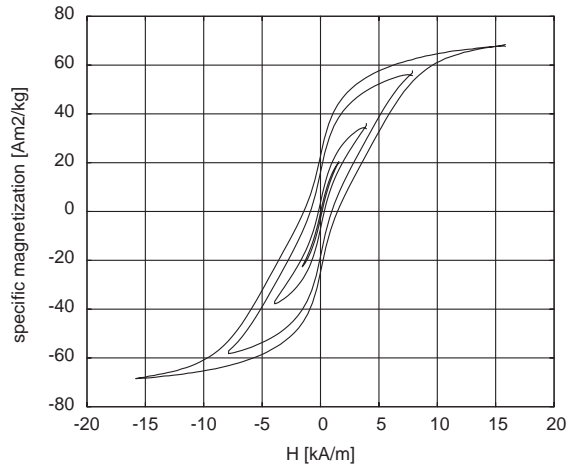


Fig. 2. Minor loops measured by VSM at room temperature for magnetosomes (sample 2) immobilised in gel (field loop amplitudes: 1.6, 4.0, 8.0 and 16.0 kA/m).

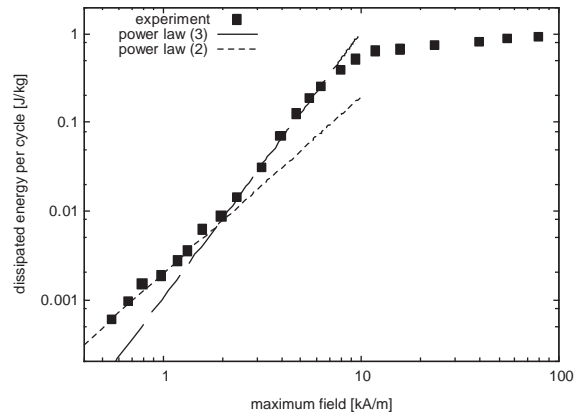


Fig. 3. Hysteresis loss of magnetosomes (sample 2) immobilised in gel in dependence on field amplitude of minor loops.

susceptibility measurements discussed below. Above the intermediary Rayleigh regime hysteresis losses increase slower with field amplitude and saturate at amplitudes above the coercivity field. Assuming for hyperthermia or thermoablation applications typical values of field amplitude of 10 kA/m and frequency 410 kHz which already proved useful in biomedical experiments [19], a value of specific hysteresis loss power of 230 W/g for sample 2 was estimated.

On samples textured in magnetic field described above magnetisation loop measurements were performed in dependence on the direction of the external magnetic field with respect to the texture axis using a constant field amplitude of 79.6 kA/m. Fig. 4 shows magnetic remanence (a), coercivity (b) and specific loss power (c) in dependence on the external magnetic field orientation. The alignment effect of particle moments may be clearly seen. In particular, the anisotropy of coercivity matches well with the theoretical model of magnetic particle chains (cf. Fig. 1.2 in Ref. [20]). Remarkably, the specific loss power calculated for the

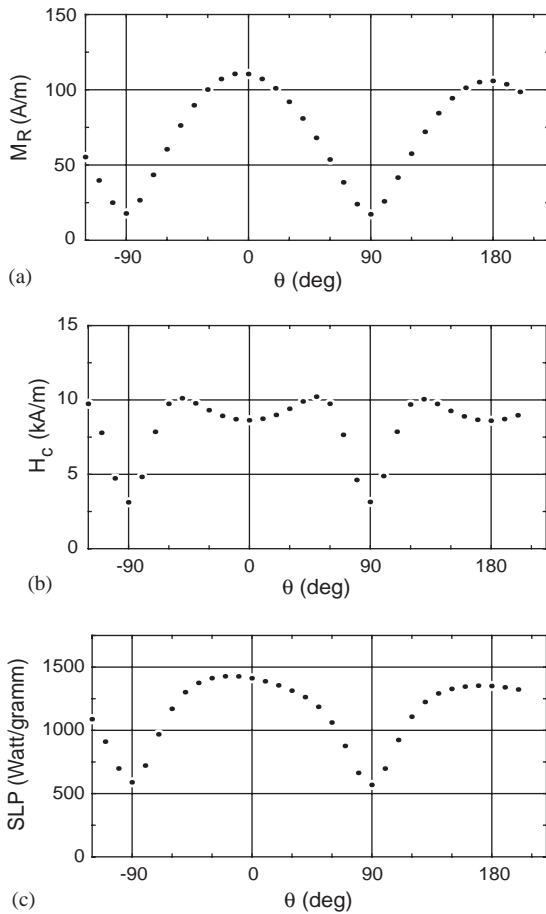


Fig. 4. Magnetic remanence (a), coercivity (b) and specific loss power at 410 kHz (c) of textured ensembles of magnetosomes in dependence on the direction of the external magnetic field with respect to the texture axis ( $\theta = 0^\circ$ ).

above-mentioned hyperthermia frequency of 410 kHz varies by nearly a factor of three reaching the extremely large value of 1400 W/g along the texture axis.

The dynamic response of the magnetosomes in frequency range 100 Hz–1 MHz was measured in alternating magnetic field of small amplitude  $< 0.1$  kA/m. Experimental details of the method are reported elsewhere [21]. Fig. 5 shows spectra of the real and imaginary part of the AC-susceptibility for aqueous suspensions of magnetosomes of sample 2. A maximum of the imaginary part of susceptibility found at 1.5 kHz is due to Brown relaxation of the magnetosomes as was shown previously [7,8]. This maximum is reduced by about an order of magnitude after immobilising the magnetosomes in gel as described above. The effect of immobilisation results in a decrease of losses at low frequencies ( $< 10$  kHz) due to elimination of the Brown relaxation path as reported early for different ferrofluids of smaller mean particle size [7,8]. Losses are unaffected by immobilisation at frequencies above about 100 kHz where viscous loss contributions are negligible.

It was found in previous investigations [7,8] for superparamagnetic ferrofluids with mean core diameters below about 20 nm that the specific loss

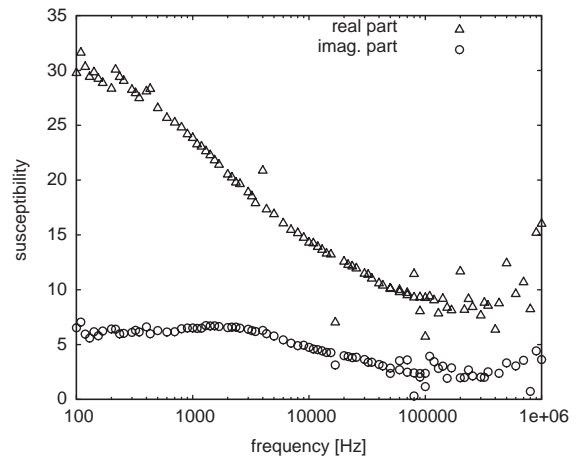


Fig. 5. Spectra of the real (triangles) and imaginary part (circles) of the AC-susceptibility for aqueous suspensions of magnetosomes (sample 1).

power  $p$  may be extrapolated from the imaginary part of susceptibility  $\chi''$  by using the well known linear small amplitude approach according to (e.g. Ref. [22])

$$p(f) = \frac{\mu_0 H^2 2\pi f}{2} \cdot \frac{\tilde{\chi}''(f)}{\rho} \quad (1)$$

( $\rho$  is the mass density of magnetic particles).

Assuming typical values of field amplitude of 10 kA/m and frequency 410 kHz mentioned above to be useful in biomedical experiments for hyperthermia and thermoablation [19], the specific loss power was estimated using Eq. (1) to be in the order of 140 and 110 W/g for liquid suspensions of sample 1 and 2, respectively. Comparison of these results with above given specific loss power data derived from hysteresis loops shows that the approximation involved in Eq. (1), while giving reasonable results for superparamagnetic ferrofluids, fails in the present case. This may be understood by the fact that the size of at least some fraction of the presently investigated magnetosomes is above the superparamagnetic regime where the square law field dependence assumed in Eq. (1) is not valid as shown by the data of Fig. 3.

To avoid difficulties with the determination of losses by using any model of magnetisation reversal, the specific loss power of the magnetosomes was measured calorimetrically at the above-mentioned field parameters used for biomedical applications (10 kA/m, 410 kHz). The experimental method was described previously [11]. Shortly, temperature increase was recorded after applying the AC-magnetic field to a sample of known heat capacity which contains the particles to be investigated. From the measured temporal temperature increase the specific loss power was calculated. At 10 kA/m and 410 kHz a value of 530 W/g is found for sample 2 and 960 W/g for sample 1. Comparing these data with our previous results found for smaller particles [7,8] the tendency of an increase of specific loss power with increasing magnetic core size (cf. Fig. 7 in Ref. [8]) is confirmed. Of course, this trend is reversed for much larger multi-domain particles (e.g. Ref. [18]). The difference of specific loss power between both present samples is mainly influenced by the difference in size distribution width, besides

being due to the difference in mean core size, too [7,16].

#### 4. Conclusions

The above described investigations of magnetic losses in magnetosomes have shown that in the transitional region between superparamagnetic and stable ferromagnetic particles difficulties with the interpretation of magnetic loss measurements may arise. Loss determination by extrapolation from experimental data of the imaginary part of the susceptibility which has been proved useful for small particles (mean core size below 20 nm) give underestimation of specific loss power in the present diameter range of particles. This is valid also for calculations from quasistatic measurements of hysteresis loops since for the present diameter range of particles, relaxation of the magnetisation during loop measurements in VSM cannot be ruled out. Obviously, the size distribution of the presently investigated particle ensembles, though rather narrow in comparison with wet chemically prepared particles, is sufficiently large that both ferromagnetic and superparamagnetic particles are present. In the case of extrapolation from the imaginary part of susceptibility the linear magnetic response assumed in Eq. (1) fails above an amplitude of about 1 kA/m where losses increase with the third power of amplitude. Consequently, extrapolation using Eq. (1) would give too low values of specific loss power. On the other hand, in the case of measurements of hysteresis loops the assumed linearity of loss power with frequency does not hold sufficiently, since particles are not large enough that relaxation during the comparatively slow VSM measurement ( $\tau_{\text{meas}} \sim 100$  s) may be neglected. As a consequence loss power derived from hysteresis loops are underestimated, too. The real magnetic losses converted into heat in hyperthermia were determined calorimetrically. The found value of 960 W/g at 10 kA/m and 410 kHz is exceptionally large in comparison to what is known from literature (e.g. Ref. [4]). Insofar, under the aspect of specific heating power magnetosomes may be regarded as

good candidates for biomedical applications in hyperthermia or thermoablation.

### Acknowledgements

The authors acknowledge support from the DFG-priority program “Colloidal magnetic liquids” under Contracts No. HE 2878/9-2, HI 698/3-2 and SCHU 1080/4-2. They thank Dr. B. Tesche and A. Dreier from MPI Kohlenforschung, Muelheim/Ruhr for TEM imaging as well as Mrs. Ch. Schmidt from IPHT for X-ray diffraction investigations.

### Note added in proof

After finishing the present paper the authors got knowledge of two papers also related to properties of magnetosomes:

R.E. Dunin-Borkowski, M.R. McCartney, M. Posfai, R.B. Frankel, D.A. Bazylinski, P.R. Buseck, *Eur. J. Mineral.* 13 (2001) 671.

A.P. Philippe, D. Maas, *Langmuir* 18 (2002) 9977.

### References

- [1] D. Schüler, *J. Mol. Microbiol. Biotechnol.* 1 (1999) 79.
- [2] U. Heyen, D. Schüler, *Appl. Microbiol. Biotechnol.* 61 (2003) 536.
- [3] P. Moroz, S.K. Jones, B.N. Gray, *Int. J. Hyperthermia* 18 (2002) 267.
- [4] W. Andrä, in: W. Andrä, H. Nowak (Eds.), *Magnetism in Medicine*, Wiley, Berlin, 1998.
- [5] I. Hilger, W. Andrä, R. Hergt, et al., *Recent Res. Dev. Radiol.* 1 (2003) 109.
- [6] R. Hergt, R. Hiergeist, I. Hilger, W.A. Kaiser, *Recent Res. Dev. Mater. Sci.* 3 (2002) 723.
- [7] R. Hergt, R. Hiergeist, I. Hilger, et al., *J. Magn. Magn. Mater.* 270 (2004) 345.
- [8] R. Hergt, R. Hiergeist, M. Zeisberger, et al., *J. Magn. Magn. Mater.* 280 (2004) 358.
- [9] M. Shinkai, M. Yanase, M. Suzuki, et al., in: U. Häfeli, et al. (Eds.), *Scientific and Clinical Applications of Magnetic Carriers*, Plenum Press, New York, 1997.
- [10] K. Grünberg, C. Wawer, B.M. Tebo, D. Schüler, *Appl. Env. Microbiol.* 67 (2001) 4573.
- [11] R. Hiergeist, W. Andrä, N. Buske, et al., *J. Magn. Magn. Mater.* 201 (1999) 420.
- [12] R.A. Mc Currie, *Ferromagnetic Materials*, Academic Press, London, 1994.
- [13] R.W. Chantrell, J. Popplewell, S.W. Charles, *IEEE Trans. Magn. MAG-14* (1978) 975.
- [14] D.C.F. Chan, D.B. Kirpotin, P.A. Bunn, in: U. Häfeli, et al. (Eds.), *Scientific and Clinical Applications of Magnetic Carriers*, Plenum Press, New York, 1997.
- [15] P. Debye, *Polar Molecules*, Dover Publications, New York, 1929.
- [16] R.E. Rosensweig, *J. Magn. Magn. Mater.* 252 (2002) 370.
- [17] S. Chikazumi, *Physics of Ferromagnetism*, Oxford University Press, Oxford, 1997.
- [18] R. Hergt, W. Andrä, C.G. d’Ambly, et al., *IEEE Trans. Magn.* 34 (1998) 3745.
- [19] I. Hilger, W. Andrä, R. Hergt, et al., *Radiology* 218 (2001) 570.
- [20] E. Blums, A. Cebers, M. Maiorov, *Magnetic Fluids*, de Gruyter, Berlin, New York, 1997, p. 18.
- [21] R. Müller, R. Hergt, M. Zeisberger, W. Gawalek, *J. Magn. Magn. Mater.*, accepted for publication.
- [22] L.D. Landau, E.M. Lifshitz, *Electrodynamics of Continuous Media*, Pergamon Press, London, 1960.